Journal of Modern Technology & Engineering
Vol.3, No.1, 2018, pp.103-112

# COMPARATIVE STUDY ON THE STRUCTURAL PROPERTIES OF MONOLAYER AND BILAYER PLASMA POLYMERIZED THIN FILMS BY FTIR ANALYSES

**M.M. Kamal[1*], A.H. Bhuiyan[2]**

[1]Department of Physical Sciences, Independent University, Dhaka, Bangladesh
[2]Department of Physics, Bangladesh University of Engineering and Technology, Dhaka, Bangladesh

**Abstract.** In this paper the Fourier Transform Infrared (FTIR) analyses have been presented to compare the structural properties of plasma polymerized pyrrole (PPPy) monolayer, plasma polymerized N,N,3,5 tetramethylaniline (PPTMA) monolayer and plasma polymerized pyrrole-N,N,3,5 tetramethylaniline (PPPy-PPTMA) bilayer thin films. A capacitively coupled parallel plate glow discharge reactor was used to deposit the thin films on to glass substrates at room temperature. The bilayer composite films were formed by using pyrrole-monomer as the parent-material and N,N,3,5 tetramethylaniline monomer was deposited in different time ratios after the pyrrole films were formed. The structural analyses by FTIR spectroscopy indicated that the monomer has undergone re-organization and the ring structure is retained during the plasma polymerization of PPPy and PPTMA monolayer thin films, and the PPPy-PPTMA bilayer thin films contain the characteristics of both of its components.

***Keywords:*** *plasma polymerization, PPPy thin film, PPTMA thin film, PPPy-PPTMA bilayer thin film, FTIR analysis.*

***Corresponding Author:*** *M.M. Kamal, Department of Physical Sciences, Independent University, Bashundhara R/A, Baridhara, Dhaka - 1229, Bangladesh, e-mail: amkamal@iub.edu.bd amkamalbd@gmail.com*

***Manuscript received:*** *20 November 2017*

## 1. Introduction

In the thin film technology, plasma polymerization has been widely accepted and is preferred owing to the desirable features of the thin films it yields. The thin films produced in this process are pinhole-free and highly cross-linked and therefore are insoluble, thermally stable, chemically inert and mechanically tough. Furthermore such films are often highly coherent and adherent to a variety of substrates including conventional polymer, glass and metal surfaces (Evsyukov *et al.*, 2001; Moser *et al.*, 1999). Due to these excellent properties they have been undertaken very actively in the last few decades for a variety of applications such as protective coatings, membranes, biomedical materials, electronic and optical devices, adhesion promoters, anticorrosive surfaces, humidity sensors, electrical resistors, scratch resistant coatings, optical filters, chemical barrier coatings, etc. Metallized surfaces of synthetic materials can be protected against corrosion with a thin polymer layer deposited by plasma polymerization.

The infrared (IR) spectroscopy has been a workhorse technique for materials analysis in the laboratory for over seventy years. An IR spectrum represents a fingerprint of a sample with absorption peaks which correspond to the frequencies of

vibrations between the bonds of the atoms making up the material. Because each different material is a unique combination of atoms, no two compounds produce the exact same infrared spectrum. IR spectroscopy deals with the interaction of infrared light with matter, measures different IR frequencies by a sample positioned in the path of an IR beam and it reveals information about the vibrational states of a molecule. When a beam of electromagnetic radiation of intensity is passed through a substance, it can either be absorbed or transmitted, depending upon its frequency, and the structure of the molecules. The resulting spectrum represents the molecular absorption and transmission, creating a molecular fingerprint of the sample. It should be noted, however, that when a spectrum is recorded using a conventional, dispersive IR spectrometer, each data point reveals the transmitted light at the respective frequency. This signal is then transformed from the *time-domain* into the *frequency-domain* in order to reveal the spectrum and because of this transformation the spectroscopic analysis is termed as Fourier Transform Infrared (FTIR) spectroscopy.

IR absorption information is generally presented in the form of a spectrum with wavelength or wavenumber as the x-axis and absorption intensity or percent transmittance as the y-axis. Transmittance, *T*, is the ratio of radiant power transmitted by the sample (*I*) to the radiant power incident on the sample ($I_0$). Absorbance (*A*) is the logarithm to the base 10 of the reciprocal of the transmittance (*T*).

$$A = \log_{10}(1/T) = \log_{10}(I_0 / I) \tag{1}$$

The transmittance spectra provide better contrast between intensities of strong and weak bands because transmittance ranges from 0 to 100% $T$ whereas absorbance ranges from infinity to zero.

## 2. Literature review

Many reports on the investigation of the structural, optical and electrical behaviors of plasma polymerized thin films are widely available in the literature. It is known that Infrared (IR) spectroscopic analysis, x-ray photoelectron spectroscopy (XPS), x-ray diffraction (XRD), scanning electron microscopy (SEM), atomic force microscopy (AFM), elemental analysis (EA), etc provide information about the chemical structure of the materials. Most plasma polymers are new kinds of materials existing in the form of a highly cross-linked and highly branched three-dimensional network. IR spectroscopic analysis provides information about the structure of plasma polymers. Akther and Bhuiyan (Akther & Bhuiyan, 2005) studied the structural and optical properties of plasma polymerized N, N, 3, 5 tetramethylaniline (PPTMA) thin film. The structural analysis from FTIR spectroscopy revealed that the PPTMA thin films contain more conjugation as compared to the TMA monomer which modifies on heat treatment. Jesch et al (Jesch *et al.*, 1966) studied the FTIR spectra of plasma polymers formed from pentane, ethylene, butadiene, benzene, styrene and naphthalene. On the basis of the structures, analyzed by FTIR spectroscopy, they concluded that whether the monomer was aromatic or olefinic or fully saturated, the plasma polymer was highly branched and cross-linked and contains identifiable saturation. Kumar et al (Kumar *et al.*, 2003) studied the structural, optical and electrical characteristics of PPPy and iodine-doped PPPy thin films and found that due to iodine doping the surface morphology of the film becomes smoother and an increase in the connectivity and continuity between the blocks of polymer chains provided an increase in conductivity.

Based on the FTIR spectra, they reported that the ring structure was retained during plasma polymerization and a chemical structure was also proposed for the PPPy thin film. Pure and iodine-doped polyaniline thin films were prepared and characterized by Joseph Mathai et al (Joseph Mathai *et al*., 2002). The FTIR spectroscopic analyses revealed that the aromatic ring and the infrared absorption features of the monomer aniline were retained in the plasma polymerized aniline. Prabhakar et al (Tamirisa *et al*., 2004) investigated on polyaniline thin films by FTIR analyses which indicated that the chemical composition and structure of the films were very dependent on the substrate's position with respect to the rf coil, there being considerably less aromatic character closer to the coil. Polylinalool thin films were fabricated using rf plasma polymerization by Kateryna Bazaka et al (Bazaka K. *et al.*, 2010). All films were found to be smooth, defect-free surfaces and the FTIR analysis of the polymer showed a notable reduction in –OH moiety and complete dissociation of C=C unsaturation compared to the monomer, and presence of a ketone band absent from the spectrum of the monomer. Kamal and Bhuiyan studied on the optical characterization (Kamal & Bhuiyan, 2011) and direct current electrical characterization (Kamal & Bhuiyan, 2012) of the plasma polymerized pyrrole-*N,N,3,5* tetramethylaniline (PPPy-PPTMA) bilayer thin films. The optical characterization (Kamal & Bhuiyan, 2013a) and direct current electrical characterization (Kamal & Bhuiyan, 2013b) of the PPPy monolayer thin films were also reported by Kamal and Bhuiyan. They also reported the DC electrical conduction mechanism (Kamal & Bhuiyan, 2014) and Temperature dependence of DC electrical conduction (Kamal & Bhuiyan, 2016) of PPPy monolayer thin films.

## 3. Experimental Details

### *3.1 Sample Preparation*

A capacitively coupled parallel plate reactor has been used to deposit PPPy, PPTMA and PPPy-PPTMA bilayer thin films on to glass substrates at room temperature. To deposit the bilayer films, pyrrole-monomer has been used as the parent-material and TMA monomer has been deposited in different deposition time ratio after the pyrrole films were formed.

The monomer pyrrole and the monomer TMA were collected from Aldrich-Chemie D-7924, Steinheim, England. The monomers vapor were introduced to the reactor through a flowmeter at the flow rate of about $20cm^3$(STP)/min into the glow discharge reactor. The glow discharge system is a bell-jar type capacitively coupled system and consists of two parallel plate electrodes of stainless steel of diameter and thickness 0.09 and 0.001m respectively and placed 0.035m apart. The glow discharge chamber was evacuated by a rotary pump (Vacuubrand, Vacuubrand GMBH & Co, Germany) and plasma was generated around the substrates, which were kept on the lower electrode, using a step up transformer connected to the electrodes with a power of about 30W at line frequency and plasma was generated around the substrates. Transparent light-yellow colored PPPy, PPTMA and PPPy-PTMA bilayer thin films of different thickness were deposited onto the glass substrates. The deposition parameters such as flow-rate, deposition-time, power, vacuum order were kept almost same for all samples so that the comparison of the results could be made for different plasma polymerized samples.

### *3.2. Fourier Transform Infrared (FTIR) Spectroscopy*

For FTIR studies, the PPPy, PPTMA and PPPy-PPTMA bilayer thin film were scraped off from the glass substrates in powder form and were mixed with potassium bromide (KBr). This mixture was then pelletized. These pellets of the mixture were used to record the FTIR spectra at room temperature using an FTIR spectrometer (Shimadzu -IR 470, Shimadzu Corporation, Tokyo, Japan). All the spectra were recorded in transmittance (%) mode in the wavenumber region 4000-500 $cm^{-1}$.

## 4. Results and discussion

### *4.1. FTIR spectra of pyrrole monomer and PPPy Thin Films*

Fig. 1 represents the FTIR spectra of pyrrole monomer and PPPy, and in the Table 1 the peak assignments for the pyrrole monomer and peak assignments for the PPPy thin films are shown.

In the FTIR spectrum of the pyrrole monomer and PPPy (Fig. 1) the absorption bands are found to be very close to those reported previously (Eufinger *et al.*,1996; John & Kumar, 2002; Kumar *et al.*, 2003). It is seen that the FTIR spectrum of the PPPy is relatively complicated than that of the pyrrole monomer. Both spectra show a strong peak at about 3383 $cm^{-1}$, which are due to the N-H bond stretching vibration of primary and secondary amines and imines (Eufinger *et al*., 1996).

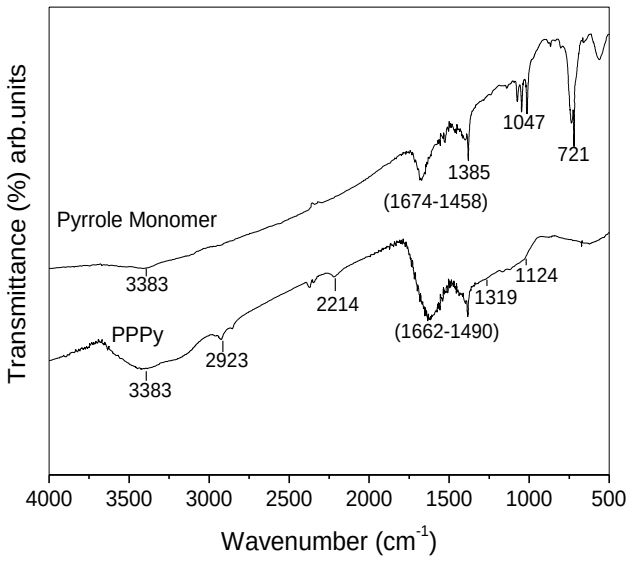


**Figure 1.** The FTIR spectra of Pyrrole monomer and PPPy.

The absorption around 1650 $cm^{-1}$ corresponds to the amines in the pyrrole structure. At about 2923 $cm^{-1}$, there is a sharp peak in PPPy spectrum but not in monomer spectrum. The peak is due to asymmetric and symmetric C-H stretching vibrations of saturated hydrocarbon. Pyrrole has highly strained ring so that the ring is easy to open under plasma polymerization. Therefore the FTIR spectrum of PPPy is very different to that of the monomer. In the molecular structure of the pyrrole monomer, all the carbon atoms are unsaturated. Thus, the peaks around 2900 $cm^{-1}$ arise

due to the plasma polymerization. There is another special peak around 720 $cm^{-1}$ appearing in the spectrum of pyrrole monomer, but not in the spectrum of PPPy. This peak usually belongs to $–CH_2–$ unites. All of these differences indicated that the monomer has undergone the re-organization during the plasma polymerization.

**Table 1.** Assignments of FTIR absorption peaks for Pyrrole monomer and PPPy

| Vibrations | Wavenumber ($cm^{-1}$) | |
|---|---|---|
| | Pyrrole | PPPy |
| **N-H** stretching vibration of primary and secondary amines | 3383 | 3383 |
| Asymmetric and symmetric **C-H** stretching vibration of saturated hydrocarbon | - | 2923 |
| **—N=C=O** | - | 2214 |
| **C=C** conjugated and **C=N** conjugated stretch and **N-H** deformation vibration | 1674-1458 | 1652-1490 |
| Alkane **C-H** deformation | 1384 | - |
| **C-N** stretching vibration | 1047 | 1124 |
| Tetra substituted Benzene | - | - |
| **C-H** out of plane bending | 721 | - |

### *4.2. FTIR spectra of TMA monomer and PPTMA Thin Films*

Fig. 2 shows the FTIR spectra of TMA and PPTMA and in Table 2 the peak assignments for TMA and PPTMA are presented.

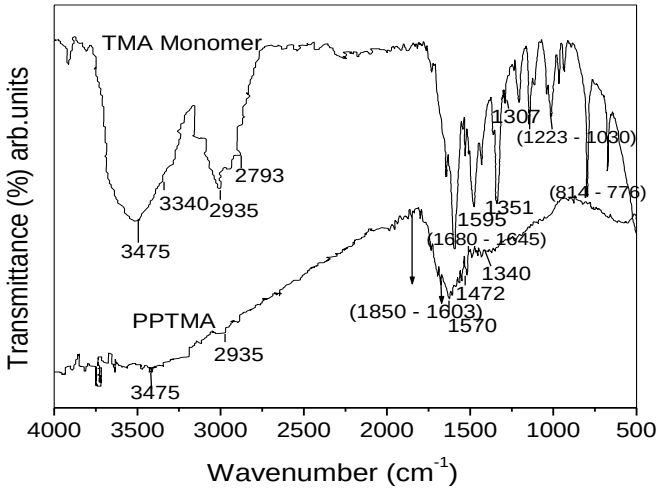


**Figure 2.** The FTIR spectra of TMA monomer and PPTMA.

Akther and Bhuiyan (Akther & Bhuiyan, 2005) reported that in this spectrum, the absorption bands at around 3435, 2935, 1850-1603, 1570, 1472 and 1340 $cm^{-1}$ in the wide absorption envelope resulting from the presence of N-H stretching vibration, C-H stretching vibration, an aromatic ring C=C stretching vibration in benzenoid and

quinoid rings and CN stretching vibration respectively (Akter & Bhuiyan, 2005). The wide band around 1850-1603 $cm^{-1}$ may also include the contribution due to C=O stretching vibration which is typical for plasma polymers. The formation of carbonyl group is usually attributed to the oxidation of the hydrocarbon part of the PPTMA after exposure to air owing to oxygen reactions with a radical species (dangling bonds) trapped in the structure of the plasma polymer. Cross-linking may also occur between different carbons of the chains due to the loss of hydrogen, particularly in the plasma-polymerized films because of the impact of energetic particles within the plasma during deposition. Here the PPTMA shows a widening of the band corresponding to the C=C stretching vibration of benzenoid and quinoid and slight down-shifting of CN stretching vibrations, probably caused by cross-linking interactions intrinsically associated with plasma polymers. The FTIR observations reveal that the PPTMA contain an aromatic ring structure with NC and CH side groups. From the above discussion it is understood that the PPTMA film deposited by the plasma polymerization technique does not exactly resemble to that of the TMA structure.

**Table 2.** Assignments of FTIR absorption peaks for TMA monomer and PPTMA

| Vibrations | Wavenumber ($cm^{-1}$) | |
|---|---|---|
| | TMA | PPTMA |
| **N-H** stretching vibration of primary and secondary amines | 3475 | 3435 |
| Symmetric **N-H** stretching vibration | 3340 | - |
| Asymmetric and symmetric **C-H** stretching vibration of saturated hydrocarbon | 2935, 2793 | 2935 |
| **C=O** | - | 1850-1603 |
| **C=C** stretching vibration | 1680-1645 | |
| **C=C** stretching vib. in benzenoid and quinoid | 1595, 1484 | 1570, 1472 |
| **C-N** stretching vibration | 1351, 1307, 1223 -1030 | 1340 |
| Tetra substituted Benzene | 814 - 776 | - |

### *4.3. FTIR spectra of PPPy-PPTMA Bilayer Thin Films*

Fig. 3 represents the FTIR spectra of the PPPy-PPTMA bilayer thin films and in Table 3 the peak assignments for the Fig. 3 is also given. For comparative study, the FTIR spectra of PPPy and PPTMA thin films are also presented in this figure.

Comparing the FTIR spectra of PPPy, PPTMA and PPPy-PPTMA bilayer films, it is seen that both the spectra exhibit a broad band between 3300 $cm^{-1}$ and 3400 $cm^{-1}$, which is due to the N-H stretching vibration of primary and secondary amines and imines (Eufinger *et al*., 1996). In the bilayer film the relative intensity of this peak is higher than that in the PPPy film. The bilayer film has a relatively more intense peak at 2924 $cm^{-1}$ compared to 2923 $cm^{-1}$ of PPPy film and 2935 $cm^{-1}$ of PPTMA films, which is due to the symmetric and asymmetric C-H stretching vibration of saturated hydrocarbons. Since the peak around 2930 $cm^{-1}$ can be attributed to the asymmetric $CH_2$ vibration, it can be suggested that the bilayer

film contains more methylene groups than the other films. In addition to this, the bilayer spectrum exhibits peak at 1384 $cm^{-1}$ which is due to the C-H deformation of a $CH_3$ group.

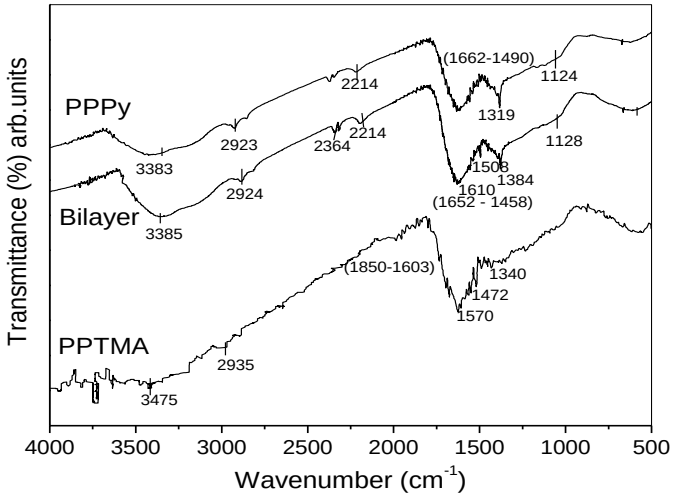


**Figure 3.** The FTIR spectra of PPPy, PPTMA and PPPy-PPTMA bilayer films.

**Table 3.** Assignments of FTIR peaks for PPPy, PPTMA and PPPy-PPTMA bilayer films

| Vibrations | Wavenumber ($cm^{-1}$) | | |
|---|---|---|---|
| | PPPy | PPTMA | PPPy-PPTMA |
| **N-H** stretching vibration of primary and secondary amines | 3383 | 3435 | 3385 |
| Asymmetric and symmetric **C-H** stretching vibration of saturated hydrocarbon | 2923 | 2935 | 2924 |
| **—N=C=O** | 2214 | - | 2214 |
| **C=O** | - | 1850-1603 | - |
| **C=C** conjugated and **C=N** conjugated stretch and **N-H** deformation vibration | 1652-1490 | - | 1652-1458 |
| **C=C** stretching vib. in benzenoid and quinoid | - | 1570, 1472 | 1610, 1508 |
| Alkane **C-H** deformation | - | - | 1384 |
| **C-N** stretching vibration | 1124 | 1340 | 1128 |

This again shows that the bilayer film contains more methylene groups than the PPPy or PPTMA films. The absorption peak at 2214 $cm^{-1}$ in both PPPy and PPPy-PPTMA films suggests the introduction of —N=C=O group (Fally *et al*, 1995) which is very typical in plasma polymerization (Westwood, 1974; Yasuda *et al.*, 1976). The absorption at 1508 $cm^{-1}$ and 1610 $cm^{-1}$ of bilayer films can be assigned to the benzoid and quinoid structures of the benzene rings in TMA. As expected, they are found due to the presence of TMA,

because pyrrole does not contain any benzene rings. This study, however, shows that the bilayer films contain the characteristics of both the monomer.

Table 4 shows the peak assignments of FTIR spectra for pyrrole monomer and PPPy, TMA monomer and PPTMA and PPPy-PPTMA together for an overall comparison.

**Table 4.** Assignments of FTIR absorption peaks for Pyrrole, PPPy, TMA, PPTMA and PPPy-PPTMA sample

| Vibrations | Wavenumber ($cm^{-1}$) | | | | |
|---|---|---|---|---|---|
| | Pyrrole | PPPy | TMA | PPTMA | PPPy-PPTMA |
| **N-H** stretching vibration of primary and secondary amines | 3383 | 3383 | 3475 | 3435 | 3385 |
| Symmetric **N-H** stretching vibration | - | - | 3340 | - | - |
| Asymmetric and symmetric **C-H** stretching vibration of saturated hydrocarbon | - | 2923 | 2935, 2793 | 2935 | 2924 |
| **—N=C=O** | - | 2214 | - | - | 2214 |
| **C=O** | - | - | - | 1850-1603 | - |
| **C=C** conjugated and **C=N** conjugated stretch and **N-H** deformation vibration | 1674-1458 | 1652-1490 | - | - | 1652-1458 |
| **C=C** stretching vibration | - | - | 1680-1645 | | - |
| **C=C** stretching vib. in benzenoid and quinoid | - | - | 1595, 1484 | 1570, 1472 | 1610, 1508 |
| Alkane **C-H** deformation | 1384 | - | - | - | 1384 |
| **C-N** stretching vibration | 1047 | 1124 | 1351, 1307, 1223 - 1030 | 1340 | 1128 |
| Tetra substituted Benzene | - | - | 814 - 776 | - | - |
| **C-H** out of plane bending | 721 | - | - | - | - |

As discussed above, a comparative study from the Table 4 between the pyrrole monomer and PPPy clearly shows characteristics differences, especially at 2923, 2214 and 721 $cm^{-1}$, which indicate that the monomer has undergone the re-organization during the plasma polymerization. In a similar comparative study between TMA monomer and PPTMA, the differences might be observed especially at 3340, 2793, 1850-1603, 1680-1645, and 814-776 $cm^{-1}$. From these differences it is indicated that the PPTMA film deposited by the plasma polymerization technique does not exactly

resemble to that of the TMA structure. Finally, comparison between PPPy, PPTMA and PPPy-PPTMA shows that the bilayer films contain the characteristics of both the monomer.

## 5. Conclusions

A comparative study of the FTIR spectra of pyrrole monomer and PPPy clearly shows characteristics differences, especially at 2923, 2214 and 721 $cm^{-1}$, which indicates that the monomer has undergone the re-organization during the plasma polymerization. The FTIR spectrum of the PPPy is relatively complicated and is very different than that of the pyrrole monomer. At about 2923 $cm^{-1}$, there is a sharp peak in PPPy spectrum but not in monomer spectrum has appeared due to asymmetric and symmetric C-H stretching vibrations of saturated hydrocarbon. The special peak around 720 $cm^{-1}$ which is seen in the spectrum of pyrrole monomer, but not in the spectrum of PPPy, is usually belongs to $–CH_2–$ unites. On the other hand the FTIR observations reveal that the PPTMA contain an aromatic ring structure with NC and CH side groups and it is understood that the PPTMA film deposited by the plasma polymerization technique does not exactly resemble to that of the TMA structure. Comparison to FTIR spectra of PPPy, PPTMA and PPPy-PPTMA bilayer films, it is seen that all the spectra exhibit a broad band between 3300 $cm^{-1}$ and 3400 $cm^{-1}$, which is due to the N-H stretching vibration of primary and secondary amines and imines. In the bilayer film the relative intensity of this peak is higher than that in the PPPy film. The bilayer film has a relatively more intense peak at 2924 $cm^{-1}$ compared to 2923 $cm^{-1}$ of PPPy film and 2935 $cm^{-1}$ of PPTMA films. Since the peak around 2930 $cm^{-1}$ can be attributed to the asymmetric $CH_2$ vibration, it can be suggested that the bilayer film contains more methylene groups than the other films. In addition to this, the bilayer spectrum exhibits peak at 1384 $cm^{-1}$ which is due to the C-H deformation of a $CH_3$ group. This again shows that the bilayer film contains more methylene groups than the PPPy or PPTMA films. The absorption at 1508 $cm^{-1}$ and 1610 $cm^{-1}$ of bilayer films can be assigned to the benzoid and quinoid structures of the benzene rings in TMA. As expected, they are found due to the presence of TMA, because pyrrole does not contain any benzene rings. This study, however, shows that the bilayer films contain the characteristics of both the monomer.

## References

Akther, H., Bhuiyan, A.H. (2005). Infrared and ultra violet-visible spectroscopic investigation of plasma polymerized N,N,3,5 -tetramethylaniline thin films. *Thin Solid Films,* 474, 14-18.

Bazaka, K., Jacob M.V. & Shanks R.A. (2010). Fabrication and Characterization of RF Plasma Polymerized Thin Films from 3,7-Dimethyl-1,6-octadien-3-ol Electronic and Biomaterial Applications. *Advanced Materials Research*, 123-125, 323-326.

Eufinger, S., Van Ooij, W.J. & Ridgway, H. (1996). DC plasma-polymerization of pyrrole: comparison of films formed on anode and cathode. *J. Appl. Polym. Sci., 61*(9), 1503-1514.

Evsyukov, S.E., Gautheron, F., Hoffken, H.W. & Born, K. (2001). Synthesis, X-ray structure, and polymerization of 1-Vinyl-3-cyanomethylimidazolium Chloride. *J. Appl. Polym. Sci.*, 82 (2), 499-509.

Fally, F., Doneux, C., Riga, J., & Verbist, J. J. (1995). Quantification of the functional groups present at the surface of plasma polymers deposited from propylamine, allylamine, and propargylamine. *J. Appl. Polym. Sci., 56*(5), 597-614.

Jesch, K., Bloor, J.E. & Kronick, P.C. (1966). Structure and physical properties of glow discharge polymers. I. Polymers from hydrocarbons. *J. Polym. Sci., A-1, Polym. Chem.*, *4*(6), 1487-1497

John, R.K., Kumar, D.S. (2002). Structural, electrical, and optical studies of plasma-polymerized and iodine-doped poly pyrrole. *J. Appl. Polym. Sci.*, *83*(9), 1856 -1859.

Joseph, M.C., Saravanan, S., Anantharaman, M.R., Venkitachalam, S., & Jayalekshmi, S. (2002). Effect of iodine doping on the band gap of plasma polymerized aniline thin films. *J. Phys. D: Appl. Phys.*, 35(17), 2206–2210.

Kamal M.M, Bhuiyan, A.H. (2011). Optical Characterization of Plasma-Polymerized Pyrrole-N,N,3,5-Tetramethylaniline Bilayer Thin Films. *J. Appl. Polym. Sci*., 121(4), 2361–2368.

Kamal M.M, Bhuiyan, A.H. (2012). Direct Current Electrical Characterization of Plasma Polymerized Pyrrole-N,N,3,5 Tetramethylaniline Bilayer Thin Films. *J. Appl. Polym. Sci.*, 125(2), 1033–1040.

Kamal M.M, Bhuiyan, A.H. (2013). Structural and Optical Characterization of Plasma Polymerized Pyrrole Monolayer Thin Films. *Advances in Optoelectronic Materials (AOM)*, 1(2), 11-17.

Kamal M.M, Bhuiyan, A.H. (2013). Thickness Dependent Direct Current Electrical Conduction in Plasma Polymerized Pyrrole Monolayer Thin Films. *Advanced Materials Research*, 741, 59-64.

Kamal M.M, Bhuiyan, A.H. (2014). Direct Current Electrical Conduction Mechanism in Plasma Polymerized Pyrrole Thin Films. *J. of Modern Science and Technology*, 2(2), 1-9.

Kamal M.M, Bhuiyan, A.H. (2016). Temperature Dependence of DC Electrical Conduction in Plasma Polymerized Pyrrole Thin Films. *J. of Modern Science and Technology*, 4(1), 36-45.

Kumar, D.S., Nakamura, K., Nishiyama, S., Ishii, S., Noguchi, H., Kashiwagi, K., & Yoshida, Y. (2003). Optical and electrical characterization of plasma polymerized pyrrole films. *J. Appl. Phys.*, *93*(5), 2705-2711.

Moser, E.M., Faller, C., Pietrzko, S., & Eggimann, F. (1999). Modeling the functional performance of plasma polymerized thin films. *Thin Solid Films*, 355-356, 49-54.

Tamirisa P.A., Liddell K.C., Pedrow P.D. & Osman M.A. (2004). Pulsed-Plasma-Polymerized Aniline Thin Films. *J. Appl. Polym. Sci.*, 93(3), 1317-1325.

Westwood, A.R. (1971). Glow discharge polymerization-I. Rates and mechanisms of polymer formation. *Eur. Polym. J.*, 7(4), 363-375.

Yasuda, H., Bumgarner, M.O., Marsh, H.C. & Morosoff, N. (1976). Plasma polymerization of some organic compounds and properties of the polymers. *J. Polym. Sci. Polym. Chem.*, 14, 195-224.